NUMERICAL CALCULATIONS AND ANALYSES IN A DIAGONAL TYPE MHD GENERATOR

Le Chi Kien

Ho Chi Minh City University of Technical Education, 01 Vo Van Ngan, Thu Duc, Ho Chi Minh City

Email: *kienlc@hcmute.edu.vn*

ABSTRACT

This study considers the affect of magnetic field on the electrical current distribution in the exit areas of a diagonal MHD generator. The 2-D analysis has been carried out and the computational calculations have been made with the working fluid of helium seeded by cesium. The result shows that the decreasing of magnetic induction can create the constant current distribution at the exit area of the channel, and only a little affect in the middle area of the channel. There is no need a large ballast resistor for the electrodes. Furthermore, the resistance of the exit area and the current distribution at the electrode align decreases with the decreasing of the magnetic induction. It is seen clearly that the output electrodes of the MHD generator should be organized in the decreasing area of the magnetic field, because it can be significant to make the electrical parameters of generator better.

Keywords: numerical calculation, MHD generator, diagonal type, two-dimensional analysis, ballast resistance.

1. INTRODUCTION

It is determined that the operation parameters of a diagonal MHD generator is nearer to those of a Faraday MHD generator by the 1-D MHD researches [1, 2]. However, this 1-D is un-convenient to treat the influence of the un-constant working plasma in the MHD channel.

By 2-D theory, this paper has considered the electrical parameters in the middle area of the channel as mentioned in [3]. Moreover, in the exit area of the channel, there is a effect that reduce the electric features.

Hence, the outlet effect in the Faraday type has been examined in [4, 5, 6]. Beside that, this effect has been studied a little in [7, 8, 9]. For that reason, this paper has considered the position effect of the electrodes and the decreasing of the magnetic field in the channel on the current distribution of the diagonal MHD generator in case of constant physical quantities as we know that the position of electrode has some influence on the current concentration [10].

This study has examined the effect at the beginning and exit area of the diagonal MHD channel by 2-D theory. The fundamentals of the boundary conditions are also studied. The

specifications of the fluid speed and the magnetic field are discussed in this paper. In the next section, the computational calculations are considered to show the influence of the magnetic field on the current concentration as well as the inside resistance in the exit area of the channel.

2. FUNDAMENTAL THEORY

2.1. Basic theory

To analyze the outlet effect in the MHD channel, we assumed that the current, electric field etc. change with x and y as described in Fig. 1, and the fluid speed and temperature depend on only y as shown in Eqs. (9) and (10). In this case, the pressure is constant.

To consider the current distribution in the MHD channel, we explain the stream parameter Ψ as:

$$J_x = \partial\Psi/\partial y, J_y = -\partial\Psi/\partial x \tag{1}$$

where J_x and J_y are the x-axis and y-axis current density, and neglect the J_z.
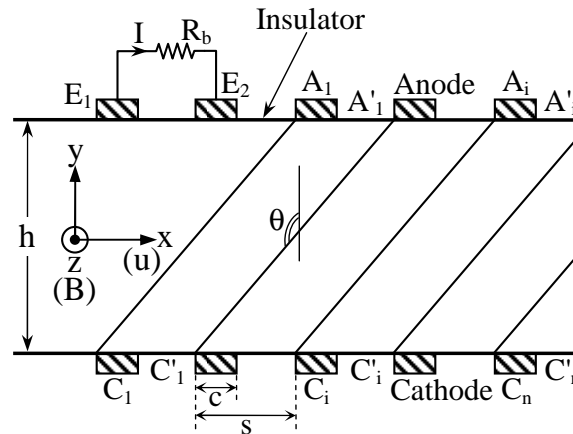
Figure 1. Cross section of the channel.

Here, the magnetic field B is only in z-axis, and the fluid velocity u is only in x-axis. From the Maxwell and Ohm law in [3], we have this equation:

$$\nabla^2\Psi + P\partial\Psi/\partial x + Q\partial\Psi/\partial y = R \tag{2}$$

where

$$
\left.
\begin{aligned}
&P = \sigma/\varepsilon\{\partial(\varepsilon/\sigma)/\partial x - \partial(\beta/\sigma)/\partial y\} \\
&Q = \sigma/\varepsilon\{\partial(\varepsilon/\sigma)/\partial y + \partial(\beta/\sigma)/\partial x\} \\
&R = \sigma/\varepsilon\{-\partial(\partial p_e/\partial y/en_e)/\partial x + \\
&\qquad +\partial(\partial p_e/\partial x/en_e)/\partial y + \\
&\qquad +u\partial B/\partial x\} \\
&\varepsilon = 1 + \beta\beta_i
\end{aligned}
\right\} \tag{3}
$$

in which e is the electron charge, $p_e = n_e kT_e$ the electron partial pressure, n_e the electron density, k Boltzmann's constant, T_e the electron temperature, β the Hall parameter for electron, β_i the

Hall parameter for ion, and σ the scalar electrical conductivity of the plasma. Because σ, β, n_e and T_e are given in [3], we do not define here.

2.2. Boundary conditions

First, the boundary condition on the electrode outward is

$$E_x = 0 \tag{4}$$

where E_x is the x-axis electric field. On the insulating wall outward

$$J_y = 0 \tag{5}$$

Using Eq. (1), these conditions (4) and (5) are transformed to

$$\varepsilon \partial\Psi / \partial y - \beta \partial\Psi / \partial x - \sigma \partial p_e / \partial x / e n_e = 0 \tag{4'}$$

$$\Psi = \text{const} \tag{5'}$$

For the diagonal MHD, the voltage difference between anode A_i and cathode C_i is shorted as seen in Fig. 1. Then, the subsidiary condition is

$$V_i = -\int_{A_i}^{C_i} E ds = 0 \, , \, I = 1, 2, \ldots, n \tag{6}$$

where E is the electric field, ds is the line between A_i and C_i, and V_i the voltage difference between A_i and C_i.

The current from area S_i between A'_i and C'_i is also the load current I, the next condition is

$$\int_{S_i} J dS = I \, , \, I = 1, 2, \ldots, n \tag{7}$$

where dS is the vector of the area S_i.

In this study, we assume that the electrical parameters are periodic with the period is the electrode pitch s behind the n-th electrode pair A_n and C_n. The last condition is

$$J(x + s) = J(x) \tag{8}$$

By Eq. (1), the Eq. (8) is transformed into

$$\Psi(x + s) = \Psi(x) + I_y^{(n)} \tag{8'}$$

where $I_y^{(n)}$ is the current flowing into A_n.

By solving Eq. (2) with the above conditions, the current distribution is expressed in section 3.

2.3. Calculation of voltage

After solving Eq. (2), E at the reference position can be found by Eq. (1). The voltage at any position can be found by the line integration of E from a optional position to the considered position.

2.4. Gas velocity and temperature distributions

The velocity u and temperature T change only in the y-axis as [11]:

$$u / u_0 = \{4y / h(1 - y / h)\}^{tm} \tag{9}$$

$$(T - T_w)/(T_0 - T_w) = \{4y/h(1 - y/h)\}^n \tag{10}$$

respectively, where h is the channel height, u_0 and T_0 are the temperature and velocity in the middle of fluid, namely $y = h/2$ and T_w is the side temperature.

2.5. Magnetic field

To apply the magnetic field B, the MHD channel should be put in the magnetic field decreasing area. To consider the influence of B, we assume that the intensity of magnetic field does not change in the middle area, and it decreases linearly from the left side of the j-th electrode in the exit areas of the channel. In this study, the six types of B are shown in Fig. 2, where g is the gradient of B and j = 5.
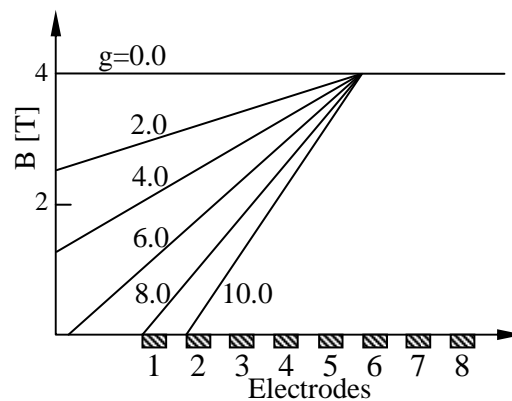
Figure 2. Configuration of magnetic field.

3. NUMERICAL SOLUTION

The solution of Eq. (3) must meet the conditions (6), (7). From (1), (7), we have

$$\Psi_i^{A'} - \Psi_i^{C'} = I/w \, , \, I = 1, 2, \ldots, n \tag{11}$$

where $\Psi_i^{A'}$ and $\Psi_i^{C'}$ are the values of Ψ on the insulating wall surfaces $A_i{'}$ and $C_i{'}$ respectively, and w is the channel width in the z-axis.

When the current I, the width w, and $\Psi_i^{A'}$ are assumed reasonable, the $\Psi_i^{C'}$ is calculated by Eq. (11). If Eq. (2) is calculated with the $\Psi_i^{A'}$, $\Psi_i^{C'}$ and suitable u, σ and β, we have the computational value of Ψ. From the Eq. (1) and the Ohm law, we have the E_x and E_y. Using these values of E_x and E_y in Eq. (6), we have the V_i and this value may be not zero.

The resistance of the electrodes A_i-C_i

$$R_i' = h/\{\langle\sigma\rangle_i \, cw \cos(\pi - \theta)\}, \, I = 1, 2, \ldots, n \tag{12}$$

where h, c and θ are the channel height, the electrode width and the angle of inclination to the y-axis, respectively, and we have an ideal current:

$$I_i = V_i/R_i' \, , \, i=1, 2, \ldots, n \tag{13}$$

704

flows through the resistance R_i'. To short V_i, run the current $-I_i$ over R_i. Then it increases by $-I_i$ the value of $w(\Psi_{i+1}^{A'} - \Psi_i^{A'})$. This gives the current flows into the anode A_i.

Continuing with the new $\Psi_i^{A'}$, we reproduce the above procedure. If V_i is small enough after this reproduction, we have the computational value of Ψ. Furthermore, the other computational solutions are expressed in [12].

4. NUMERICAL CALCULATION

4.1. Conditions

Computational calculation is used for the MHD channel with mixture working fluid of cesium-helium in non-equilibrium plasma in which

$$\left.\begin{array}{l} h = 0.2, s = 0.1, w = 0.1, c = 0.06\,m \\ T_0 = 1800\,K, T_w = 1600\,K, p = 5\,atm \\ u_0 = 2000\,m/s, m = n = 1/7, B_0 = 4\,or\,5\,T \\ \delta = 5, \varepsilon_s = 0.3\% \end{array}\right\} \tag{14}$$

where ε_s is the seed fraction of C_s, B_0 the magnetic field in the middle area of channel, and δ the collision loss factor. These values are referred to a MHD generator of the power plant [13]. The load current runs into two electrodes E_1 and E_2 with the same value through a resistor R_b given by (see Fig. 1).

$$R_b = -\int_{E_1}^{E_2} Eds/(I/2) \tag{15}$$

Here, the R_b is called a ballast resistance.

4.2. Results

Figs. 3a~3c show the current concentrations when $g = 0$, 6 and 10 T/m, respectively, $B_0 = 4$ T and $I = 70$ A with the outline gap current is 1/20 of the load current. In the figures, $\langle J \rangle_{el} = 0.583$ A/cm^2, $\langle \sigma \rangle = 1.84$ mho/m, $\langle \beta \rangle = 2.01$ and $\beta_{crit} = 2.48$, where $\langle J \rangle_{el}$ is the mean current density of the electrodes, $\langle \beta \rangle$ and $\langle \sigma \rangle$ are the Hall parameter and mean electrical conductivity in the middle of fluid, respectively, β_{crit} is the critical Hall parameter [14].

In Fig. 3a, the current distribution in the outline of the electrodes is very strong when B does not change. Conversely, Figs. 3b and 3c show that the distribution is small when B decreases much more becauseβ is small at the region effected by a space decreasing of B. From these figures, we have also seen that the current running into the diagonal electrodes decreases with the increasing of the B gradient at the inlet area of channel. As details, the current of 60, 25, 15 % of load current run into C, when $g = 0$, 6 and 10 T/m, respectively. These figures also show that the eddy current does not appear when the electrodes are arranged in the decreasing area of magnetic field [5], and that electrode disposing with the decreasing area of B does not affect on the current distribution in the middle area of the channel.

Figure 4 indicates the changing of the voltage difference of A_1-C_1~A_8-C_8 versus E_1 electrodes. It shows that the great voltage difference appears between E_1 and E_2 electrode when the magnetic field B does not decrease ($g = 0$). In the other cases, the voltage difference

decreases when g increases, and it nearly disappears when g=6, and the opposite difference arises when g > 7. This figure also shows that the voltage difference in the middle area of the channel is less affected by the decreasing of magnetic field.

(a) g=0, B_0=4

(b) g=6, B_0=4

(c) g=10, B_0=4
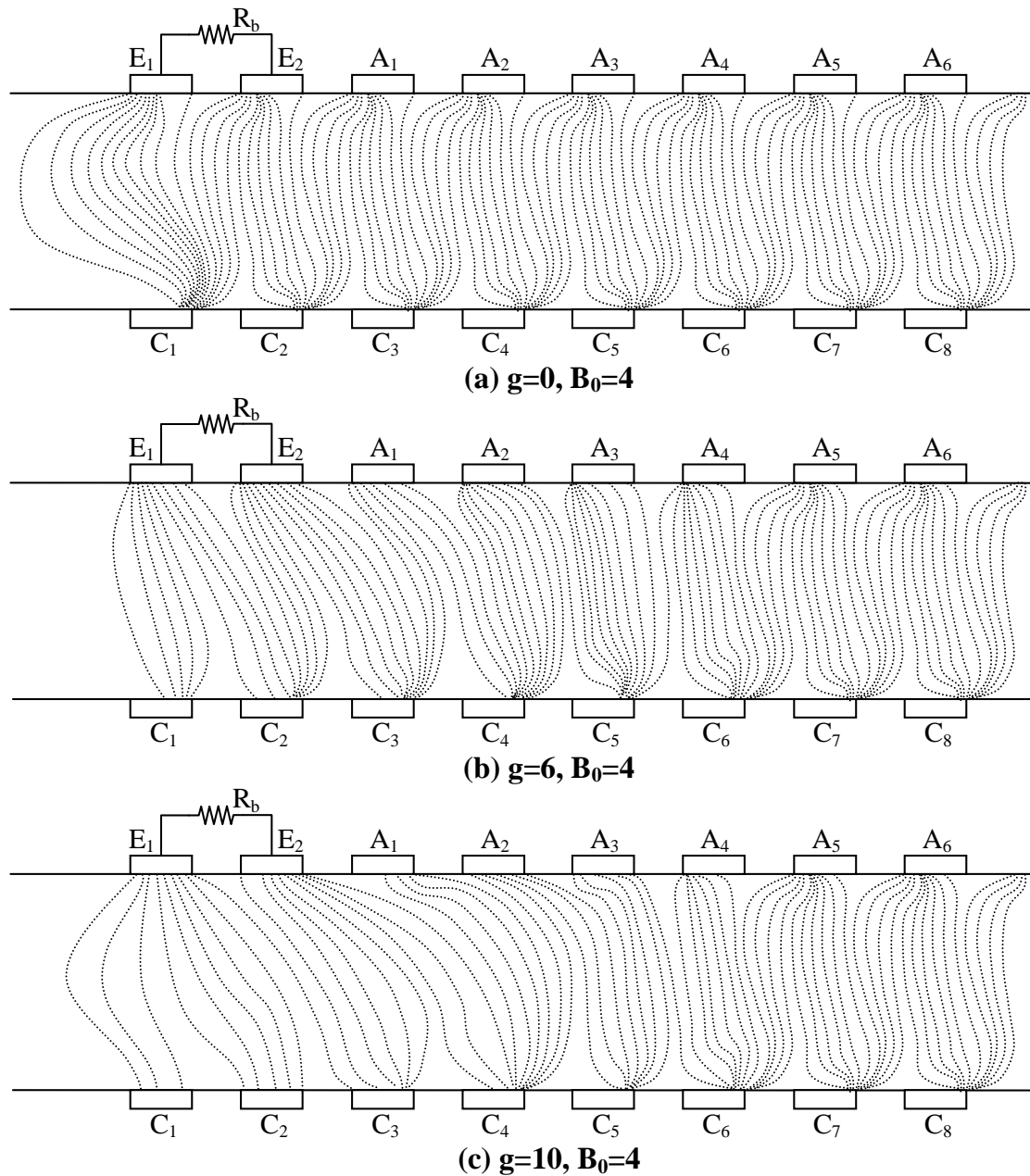
Figure 3. Current concentrations.

To evaluate the outlet effects of the MHD generator, this paper considers the inside resistance R_i of the exit area and the level of the current distribution on the electrodes described by the equations

706

$$R_i = (V_0 - V)/I \tag{16}$$

$$J_{peak}/\langle J \rangle_{el} \geq 1 \tag{17}$$

where V and V_0 are voltage difference with load and without load between the electrode E_1 and the n-th electrode, respectively, and J_{peak} is the peak current density on the electrodes. In this configuration, $J_{peak}/\langle J \rangle_{el} = 1$ indicates the status without current distribution and $J_{peak}/\langle J \rangle_{el} \gg 1$ denotes the large current distribution.
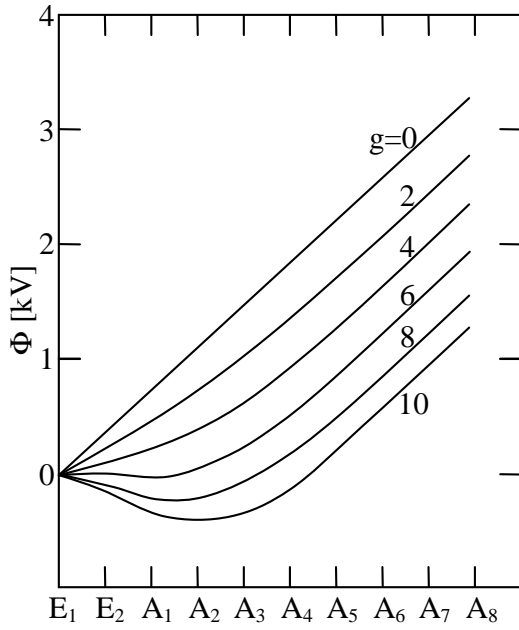
Figure 4. Variation of voltage difference for $B_0 = 4$.
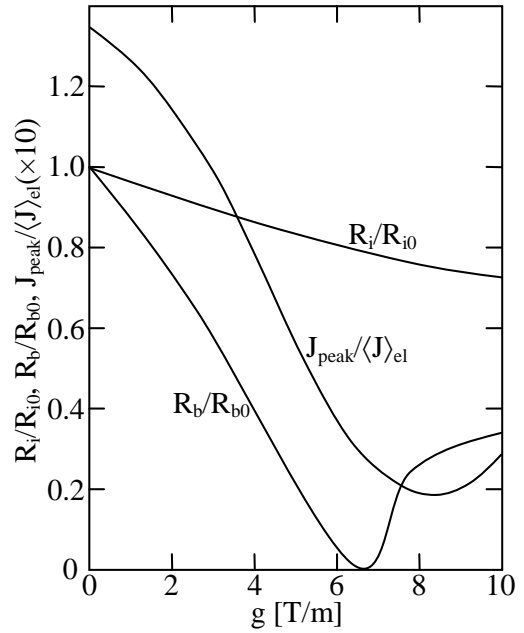
Figure 5. Influence of g on R_i/R_{i0}, R_b/R_{b0} and $J_{peak}/\langle J \rangle_{el}$ when $B_0 = 4$.
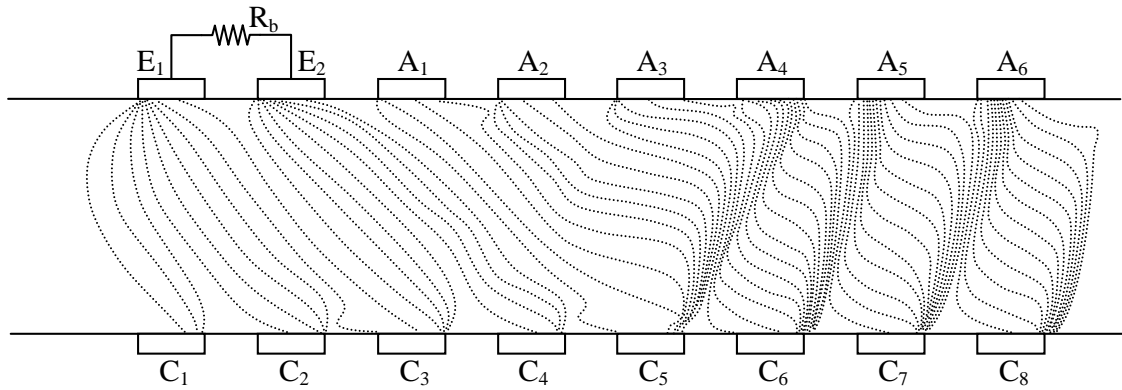
Figure 6. Current concentration for $g = 6$ and $B_0 = 5$.

Figure 5 indicates the change of R_i/R_{i0}, R_b/R_{b0} and $J_{peak}/\langle J \rangle_{el}$ versus g, where R_{b0} and R_{i0} are R_b and R_i for $g = 0$, respectively. We can see that R_i decreases with g, for example the value of R_i for $g = 6.0$ achieves about 80 % of that of R_{i0}, and that $J_{peak}/\langle J \rangle_{el}$ decreases from $g = 0$ to 8 T/m, obtains the lowest value of 1.90 and rises again. This means the current distribution at the

align of electrode reduces when g = 8 T/m. Therefore, organizing the electrodes in the decreasing area of magnetic field is significant to protect the electrodes. This figure also shows that R_b/R_{b0} decreases with g, and nearly zero when g = 6.5 and then increases with g. This means more electrodes are used, larger ballast resistors we need when magnetic field does not decrease or is over 8. However, if g = 6~7 T/m, there is no need large ballast resistors.

Figure 6 shows the current concentration in case of g = 6 T/m, B_0 = 5 T and I = 150 A, $\langle J \rangle_{el}$ = 1.25 A/cm^2, $\langle \sigma \rangle$ = 2.85 mho/m, $\langle \beta \rangle$ = 2.48 and β_{crit} = 1.90. It is seen that the fluid is effected in the middle area of channel, while the current concentration is continually constant when magnetic field decreases following the channel and the distribution is nearly moved far the electrodes. As a result, organizing the electrodes in the decreasing area of magnetic field is significant when the induction is produced in the middle area of the channel.

5. CONCLUSIONS

The main results from the above analyses are concluded as:

(1) A reasonable concentration of magnetic field can create the current concentration quite stable and constant at the exit area of the channel both when the fluid is effected and not effected in the middle area.

(2) Organizing the electrode in the decreasing area of magnetic field causes less changing in the current concentration at the middle area of the channel.

(3) If the electrode are organized in the area with a reasonable magnetic field, the voltage difference and the ballast resistor of the electrode is quite small. Therefore, a number of electrodes can be applied without great ballast resistors.

(4) The inside resistor in the exit area of the channel decreases with the decreasing of the magnetic field.

(5) The current distribution in the align of electrode can be dismissed by the decreasing of magnetic field.

As a result, the electrodes of this type of MHD generator should be organized in the area of the decreasing of magnetic field, because it can be significant to make the electrical parameters of generator better.

REFERENCES

1. Yamaguchi H., Hisazumi Y., Asano H., Morita H., Hori T., Matsumoto T., and Abiko T. - A New Heat Supply System of Cogeneration for the Local Community, JSME Journal of Power and Energy Systems **2** (3) (2008) 1085-1095.

2. Hamada Y., Amazawa K., Murakawa S., Kitayama H., Nabeshima M., and Takata H. - Study on Operation Characteristics and Performance Evaluation of Residential Combined Heat and Power System, JSER 27th International Conference on Energy, Economy, and Environment **7-1** (2011) 453-458.

3. Mori S., Akatsuka H., and Suzuki M. - Numerical Analysis of Carbon Isotope Separation by Plasma Chemical Reactions in Carbon Monoxide Glow Discharge, Journal of Nuclear Science and Technology **39** (6) (2002) 637-646.

4. BityurinV. A. - MHD Electrical Power Generation in a T-Layer Plasma Flow, IEEE Transactions on Plasma Science **28** (3) (2000) 1020-1028.

5. Aithal S. M. - Shape Optimization of a MHD Generator Based on Pressure Drop and Power Output Constraints, International Journal of Thermal Sciences **47** (6) (2008) 7 78-786.

6. Aithal S. M. - Characteristics of Optimum Power Extraction in a MHD Generator with Subsonic and Supersonic Inlets, Energy Conversion and Management **50** (3) (2009) 765-771.

7. Anwari M., Sakamoto N., Hardianto T., Kondo J., and Harada N. - Numerical Analysis of Magnetohydrodynamic Accelerator Performance with Diagonal Electrode Connection, Energy Conversion and Management **47** (13-14) (2006) 1857-1867.

8. Motoo Ishikawa, Fumiki Inui, Juro Umoto - Fault Analysis of a Diagonal Type MHD Generator Controlled with Local Control Circuit, Energy Conversion and Management **40** (3) (1999) 249-260.

9. Bhadoria B. S., and Chandra A. - Transient Analysis of Proposed Indian MHD Channel, Energy Conversion and Management **42** (8) (2001) 963-966.

10. Inui Y., Ito H., and IshidaT. - Two Dimensional Simulation of Closed Cycle Disk MHD Generator Considering Nozzle and Diffuser, Energy Conversion and Management **45** (13-14) (2004) 1993-2004.

11. Gelfgat Y., Krūminš J., and Li B. Q. - Effects of System Parameters on MHD Flows in Rotating Magnetic Fields, Journal of Crystal Growth **210** (4) (2000) 788-796.

12. Braun E. M., Mitchell R. R., Nozawa A., Wilson D. R., Lu F. K., and Dutton J. C. - Electromagnetic Boundary Layer Flow Control Facility Development Using Conductive Nanoparticle Seeding, 46th Aerospace Sciences Meeting and Exhibit, AIAA Paper **2008-1396** (2008) 11-20.

13. Chen Lingen, Gong Jianzheng, Sun Fengrui, and Wu Chih - Heat Transfer Effect on the Performance of MHD Power Plant, Energy Conversion and Management **43** (15) (2002) 2085-2095.

14. Sawaya E., Ghaddar N., and Chaaban F. - Evaluation of the Hall Parameter of Electrolyte Solutions in Thermosyphonic MHD Flow, International Journal of Engineering Science **40** (18) (2002) 2041-2056.

TÓM TẮT

NHỮNG TÍNH TOÁN SỐ VÀ PHÂN TÍCH TRONG MÁY PHÁT ĐIỆN TỪ THỦY ĐỘNG LOẠI ĐIỆN CỰC CHÉO

Lê Chí Kiên

Đại học Sư phạm Kỹ thuật TP.HCM, 01 Võ Văn Ngân, Q. Thủ Đức, TP. Hồ Chí Minh

Email: *kienlc@hcmute.edu.vn*

Bài báo nghiên cứu ảnh hưởng của sự suy giảm cảm ứng từ đến sự phân bố dòng trong vùng cuối ống phóng của máy phát điện Từ thuỷ động (MHD) loại điện cực chéo dùng plasma không cân bằng bằng phân tích hai chiều. Những tính toán trên máy tính đã được thực hiện trong trường hợp chất khí là helium được cấy bởi cesium. Kết quả là một sự suy giảm cảm ứng từ

thích hợp sẽ làm phân bố dòng điện rất đồng nhất ở gần vùng cuối ống phóng của máy phát điện đồng thời ảnh hưởng ít tới phân bố dòng điện ở vùng trung tâm của máy phát, và điện cực ngõ ra có thể được dùng mà không cần điện trở chấn lưu lớn. Thêm nữa, điện trở nội của vùng cuối và sự tập trung của dòng điện tại mép điện cực ngõ ra giảm theo sự suy giảm của mật độ từ thông. Theo nghiên cứu đây, điện cực ngõ ra của máy phát MHD loại điện cực chéo dùng plasma không cân bằng nên được đặt trong vùng suy giảm của cảm ứng từ bởi vì khi đó sẽ có lợi để cải thiện những thuộc tính điện của máy phát MHD.

Từ khóa: tính toán số, máy phát MHD, điện cực chéo, phân tích hai chiều, điện trở chấn lưu.